ICC
Iranian Chemical Communication
Original Research Article
Payame Noor University http://icc.journals.pnu.ac.ir

Molecular docking studies on xanthohumol derivatives as novel anticancer agents

Mohsen Oftadeh[a,*], Masood Fereidoonnezhad[b], Mina Aliyan[a], Fariba Aliyan[c]

[a]*Chmistry Department, Payame Noor University, 19395-4697 Tehran, I. R. Iran*

[b]*Research Center of Marine Pharmaceutical Science, Ahvaz Jundishahpour University of Medical Science, Ahvaz, Iran*

[c]*Department of Medicinal Chemistry, School of Pharmacy, Ahvaz Jundishapur University of Medical Sciences, Ahvaz, Iran*

Received: 23 January 2019, Accepted: 11 March 2019, Published: 1 July 2019

Abstract

A set of Xanthohumol derivatives were selected and molecular docking studies of these compounds on thioredoxin reductase were conducted. Based on new structural patterns using in silico-screening study, new potent lead compounds were designed. The results due to the validated docking protocols lead to find that Thr58, Gly57, Gly21, Asp334, Glu163, Ala130, IIe332, Val44 and Gly132 are the main amino acids in the active site cavity in charge of the essential interactions with thioredoxin reductase.

Keywords: *In silico*-screening; xanthohumol; cytotoxicity activity; molecular docking; thioredoxin reductase; active site cavity.

Introduction

Xanthohumol, Xn has been considered as a "broadspectrum" anticancer agent. Some putative mechanisms have been reported that show the effect of Xn on generation of reactive oxygen species, ROS [1-4], down regulation of antiapoptotic proteins [5-8], upregulation of p53 [9, 10], and induction of phase II enzymes [11, 12]. Despite the anticancer activity of Xn that is well-documented, its efficacy is moderate, and therefore, it is of demand to improve the potency of Xn for future development.

Thioredoxin, Trx, incorporated with thioredoxin reductase, TrxR, and nicotinamide adenine dinucleotide phosphate, NADPH, including the thioredoxin system, were defined by Peter Reichard and his colleagues in 1964 as a hydrogen donors for enzymatic synthesis of cytidine deoxyribonucleoside diphosphate by ribonucleotide reductase from Escherichia coli [13].

Also, enzyme purification may produce a very pure TrxR as a flavoprotein with an activity-reducing activity of the active site in the oxidized Trx [14]. The sequence of E. coli Trx1 was discovered with 108 amino acid residues in 1968 [15], suggesting that the active global activated site, Cys-Gly-Pro-Cys [16] developed anticancer drugs for thioredoxin reductase selenoprotein, TrxRs, as adsorption targets [17]. The thioredoxine system

*Corresponding author: Mohsen Oftadeh
Tel: +98 (313) 3521022, Fax: +98 (313) 3521802
E-mail: m_oftadeh@pnu.ac.ir

eventually acts as a donor to reduce equivalents for various biological processes.

In order to regulate cellular needs, the redox metabolism is required by TrxR as a part of the main regulator system of the thiol. Therefore, with changes in the level of regeneration, a pars pro toto is proposed for the whole cell. TrxR levels have been increased by many tumor cells as TrxR plays an important role in drug resistance. Accordingly, inhibition of TrxR and its related redox reactions may lead to successful treatment of a combined or cancerous cell [18].

In this work, molecular docking simulations [19] as a part of the drug design methodology have been applied for a set of Xanthohumol analogues, Xns, which are able to inhibit TrxR. This study was done in order to design new potent lead compounds based on new structural patterns used in silico-screening study, and to find the main amino acids in the active site cavity in charge of the essential interactions with thioredoxin reductase.

All compounds of the dataset and the designed ones were considered to achieve their detailed molecular binding site in intercalating with major amino acids in the active site of TrxR. A validated molecular docking simulation technique was also investigated.

Materials and methods

Data set

For this study, a dataset including 39 Xn derivatives was selected as a series of potent dual drug inhibitors such as TrxRs [13]. Table 1 shows the structural characteristics and details of the biological activity of these compounds.

Table 1. Chemical structure of the titled compounds and their experimental and cross-validated predicted activity as well as their docking binding energy of TrxRs

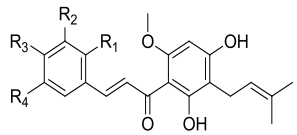

8a-8m

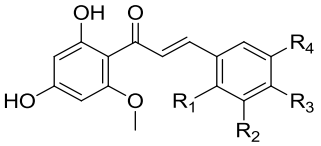

11a-11n

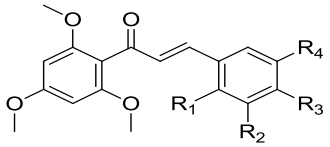

13a-13q

Name	R1	R2	R3	R4	TrxRS pIC50 (exp)	TrxRS pIC50 (pred)	TrxRS ΔG_{bind}[1] (kcal/mol)
8a	H	H	OH	H	4.4559	4.7260	-9.93
8b	H	H	OMe	H	4.4895	4.7019	-9.36
8c	H	OMe	OH	H	4.6635	4.6276	-9.62
8d	H	OH	OH	H	4.8182	4.476	-9.25
8e	OMe	H	H	H	4.8356	4.8543	-9.57
8f	H	OMe	OMe	H	4.8601	4.7469	-9.48
8g	OMe	OMe	OMe	H	4.8297	4.8098	-9.42
8j	H	H	Cl	H	4.9957	5.0850	-9.74
8k	H	H	NO_2	H	4.9066	5.0334	-9.22
8l	H	H	CF_3	H	5.8171	5.3198	-9.96

8m	H	NO2	H	H	4.7799	4.7458	-8.98
11a	H	H	OH	H	4.3958	4.4808	-8.16
11b	H	H	OMe	H	4.7423	4.6671	-8.62
11c	OMe	H	H	H	4.8153	4.8932	-8.10
11f	H	OMe	OMe	H	4.7328	4.8757	-7.92
11g	H	OMe	H	H	4.7545	4.7900	-8.60
11h	OMe	H	OMe	OMe	4.7282	4.7611	-7.90
11i	H	OMe	OMe	OMe	4.6904	4.7386	-8.06
11j	H	OH	OH	OH	4.5421	4.5103	-7.91
11k	H	H	Cl	H	4.9136	5.0039	-9.22
11l	H	H	NO_2	H	4.3872	4.6364	-7.95
11m	H	H	CF_3	H	4.8508	4.9719	-7.84
11n	H	NO2	H	H	4.7878	4.9830	-8.04
13a	H	H	OH	H	4.4318	4.5230	-8.30
13b	H	H	OMe	H	4.8697	4.7321	-8.18
13c	OMe	H	H	H	4.7878	4.8724	-8.15
13d	H	H	Me	H	4.7352	4.7709	-8.22
13e	H	OH	OH	H	4.7696	4.4073	-7.95
13f	H	OMe	OH	H	4.7696	4.7043	-8.02
13g	H	OMe	OMe	H	4.9355	4.8499	-7.95
13h	H	OMe	H	OMe	5.0458	4.8825	-8.73
13i	H	OMe	OMe	OMe	4.7825	4.7246	-7.81
13j	OMe	H	OMe	OMe	4.6234	4.7272	-8.63
13l	H	H	NO_2	H	5.0269	5.1615	-7.51
13m	H	H	CF_3	H	5.0132	5.0571	-7.97
13n	H	NO_2	H	H	5.3098	5.1450	-8.90
13o	H	H	Cl	H	4.9066	4.9216	-8.24
13p	NO2	H	H	H	5.1024	4.9352	-8.02
13q	H	H	NH_3	H	4.3449	4.3937	-8.55

[1] docking free binding energy

Docking procedure

Molecular docking was performed using Autodock 4.2 by applying an in-house batch script (DOCKFACE) [20, 21]. Each ligand was tested in the minimization methods MM+ and AM1 using HyperChem8.0 [22]. The partial charges of atoms were made by the Gasteiger-Marsili method used in the Autodock toolkit [23]. Using mgltools 1.5.6, the output structure has been changed to PDBQT, having non-polar hydrogen from merged compositions and rotating bonds [23].

From the database protocol, the TrxR three-dimensional structure (PDB ID: 3QFB) was retrieved (http://www.rcsb.org/pdb/home/home.do). All of the water molecules were removed, the lost hydrogen was added

and, after identifying the Kollman united atom charges, non-polar hydrogens were connected using autodock tools. The desolvation parameters were assigned to each protein atom, and the final process of the Lamarckian genetic algorithm [24, 25], which is commonly used in the genetic algorithm, is applied which is one of three different search algorithms performed by Autodock4.2. Accordingly, using the MGLTOOLS 1.5.6, the enzyme was converted to PDBQT.

A maximum number of 2,500,000 energy evaluations, 150 population size, 27000 maximum generations, 100 run, a gene mutation rate of 0.02 and a crossover rate of 0.8 were used for Lamarckian GA. By autogrid tools of autodock 4.2, the grid maps of the receptors were calculated. The active site and considerable proteins of the encircling surface form the size of grid in which the center of the ligand in the complex with a spacing of 0.375Å for 3QFB and there was a grid box of 60×60×60 points in x, y and z directions. Number of points in x, y and z was 61.902, -97.953 and 38.467 and for 3UT5 was -19.934, 131.986 and 116.717, respectively. Gpf and dpf files were produced by autodock tools in order to obtain the grid and docking parameter files. Based on the docked results, cluster analysis was applied by a root mean square deviation (RMSD) tolerance of 2Å. A viewer was observed co-crystal ligand within pdb file of TrxR (3QFB) and treated as other ligands. All the docking protocols were done on validated structures with RMSD values below 2 Å. By using autodock tools program (ADT, Version 1.5.6) and based on docking results, VMD software [26] and pymol molecular graphics program, ligand-receptor interactions was detected [27].

Results and discussion

To elucidate the component interactions and to obtain some insight into their molecular binding mode with TrxR, molecular docking simulations were done on 39 compounds of dataset, Table 1, and also 70 designed compounds, Table 2. Tables 1 and 6 contain the results from molecular docking that have the estimated free binding energy values (ΔG_{bind}, in $kcalmol^{-1}$) for the best position of the docked compounds, and the corresponding favorable interactions with the key amino acid residues at the active site of tubulin. Some examples are depicted in Figure 1. For TrxRs, the ΔG_{bind} values of the best docked containing of the compounds are from -7.51 to -9.96 $kcalmol^{-1}$ (Table 1). The best docking binding energies in binding to TrxRs are belong to the compound 8l. As it was shown in Table 2, the best docked poses of designed compounds are from -7.72 to -10.36 $kcalmol^{-1}$. The compound 30 shows great docking binding energies to TrxR compared to the others.

Types of the interaction of these compounds to their targets were also investigated in Figure 1. The interaction of 8a which can deduce the OH group in the para ring of **A** forms a donor hydrogen bonded with the amino acid of Asp334. Through the carbonyl group, the bridge section, in its own structure acceptor receives the hydrogen bond with the amino acids Gly57, Gly21, Ser22 and Thr58.

For 8f, the ortho ring position **A** is formed by the OH group of the para position and through the OH group of the Thr58 and Asp42 amino acids, respectively, and it is provide the donating hydrogen bond. Also the acceptor hydrogen bond is formed between methane-ring **B** and the Asp324 amino acid, and a hydrogen

bond is formed between meta-ring **B** in the methoxy group as para-positioned and the Gly162 amino acid. The carbonyl baridge group, with the amino acids Thr58 and Gly162, receives the hydrogen bond. For 30, through the group **A** of its parenil group establishes a hydrogen bond with the Asp42 amino acid. Through the methoxy group in the ortho position of the ring **A**, the amino acids of the Asp42 and Phe43 form a bonded donner hydrogen bond. Through the OH group of para ring **B**, the Ala130 Gly132 amino acids provide a donner and acceptor hydrogen bond, respectively. For 67, through the **B** ring with the amino acid group Gly21 provides hydrogen bonding. The carbonyl bridge group with the amino acid Thr151 makes an acceptor hydrogen bond. The acceptor hydrogen bond is formed through methoxy groups in the ortho position with the Leu41 amino acid and between para ring of **A** and the Thr45 amino acid, as well as through the dual bond in the bridge between the two rings, with the amino acid asp42 of the hydrogenated linker establishes.

Table 2. Structural modification of the studied compounds, their predicted activities, and docking binding energies for TrxRS inhibitory based on FA- MLR equation

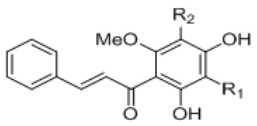

1-15

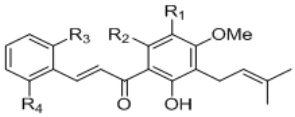

16-22

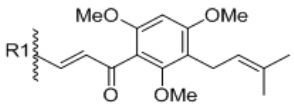

23-40

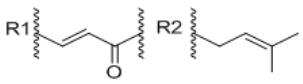

41-60

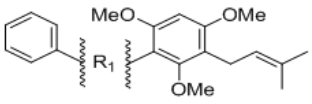

61-70

Name	R1	R2	R3	R4	QSAR [28]		Docking
					pIC_{50} Pred.	leverage	ΔG_{bind} (kcal/mol) TrxRS
1	CH3	H	-	-	4.6693	0.1043	-8.45
2	CH2-CH3-	H	-	-	4.8799	0.1909	-8.75
3	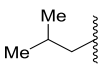	H	-	-	4.8904	0.3273	-8.79
4	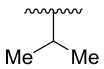	H	-	-	5.0678	0.4655	-9.48
5		H	-	-	5.2361	0.4907	-8.98
6		H	-	-	4.7305	0.1530	-8.79
7		H	-	-	4.5673	0.1268	-8.57

8		H	-	-	4.6685	0.1877	-8.78
9		H	-	-	4.7078	0.2055	-8.53
10	F	H	-	-	4.6968	0.0372	-8.04
11	Cl	H	-	-	5.0258	0.0724	-8.61
12	NO_2	H	-	-	4.8418	0.0421	-7.82
13	F	F	-	-	4.8889	0.1522	-7.84
14	F	OH	-	-	4.6662	0.0638	-8.10
15	CH_3	F	-	-	5.0768	0.0590	-8.50
16	OH	OH	OMe	OMe	4.8061	0.0582	-9.31
17	NO_2	Me	OH	OH	5.1178	0.1623	-8.52
18	F	Me	F	F	5.5295	0.3348	-8.40
19	Cl	Me	Me	F	6.1068	0.6559	-9.70
20	H	H	OH	OH	4.5404	0.1068	-8.60
21	CH_3	CH_3	Cl	OH	5.5927	0.4506	-9.67
22	OMe	OH	OMe	OMe	4.7982	0.0930	-8.36
23		-	-	-	4.9522	0.1214	-9.00
24		-	-	-	4.9177	0.1260	-8.71
25		-	-	-	4.8794	0.1202	-8.93
26		-	-	-	5.0460	0.1005	-9.60
27		-	-	-	5.0458	0.1005	-9.17
28		-	-	-	4.8245	0.0290	-8.68
29		-	-	-	4.9072	0.0877	-8.95
30	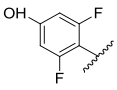	-	-	-	5.0406	0.0709	-10.36
31	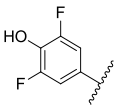	-	-	-	4.9818	0.0810	-9.00
32		-	-	-	4.9220	0.1268	-9.01

33	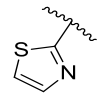	-	-	-	4.9778	0.1230	-8.70
34	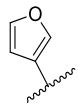	-	-	-	4.9321	0.0927	-8.44
35	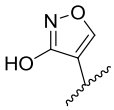	-	-	-	4.9731	0.1129	-8.96
36	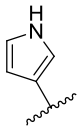	-	-	-	4.7562	0.1054	-9.03
37	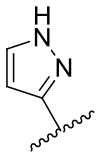	-	-	-	5.0846	0.1806	-8.66
38	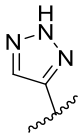	-	-	-	5.2512	0.2154	-8.54
39	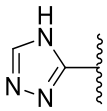	-	-	-	4.9572	0.2088	-8.84
40	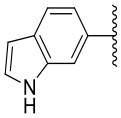	-	-	-	4.5415	0.1046	-9.98
41		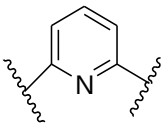	-	-	5.0862	0.5204	-8.78
42	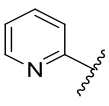	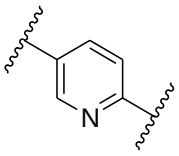	-	-	5.0673	0.3443	-8.83
43	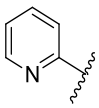	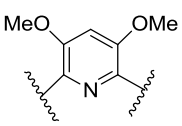	-	-	5.2046	0.3027	-9.12
44		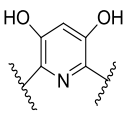	-	-	5.0973	0.2738	-8.93

45	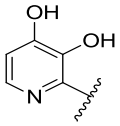	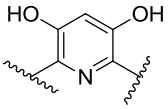			4.7239	0.0912	-8.62
46	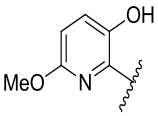	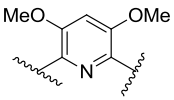	-	-	5.3088	0.2278	-9.03
47	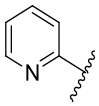	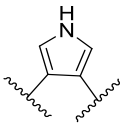	-	-	4.8576	0.4510	-8.41
48	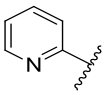	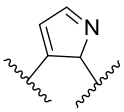	-	-	5.0255	0.4898	-8.13
49	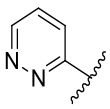	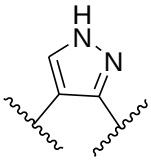	-	-	5.3779	0.4533	-8.56
50	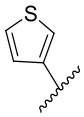	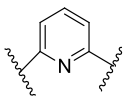	-	-	5.0688	0.5120	-8.84
51	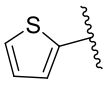	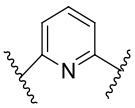	-	-	4.9946	0.4784	-8.99
52	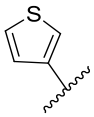	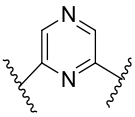	-	-	5.0176	0.3438	-8.50
53	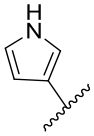	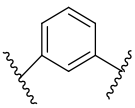	-	-	4.6710	0.5029	-9.04
54	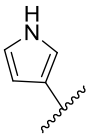	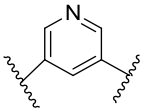	-	-	4.5261	0.3850	-8.90
55	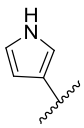	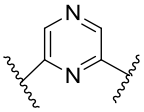	-	-	5.0911	0.5128	-8.29

56	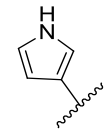	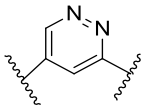	-	-	4.9886	0.3944	-9.00
57	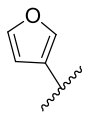	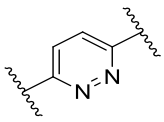	-	-	5.2817	0.4671	-8.14
58	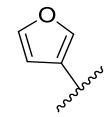	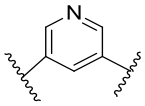	-	-	4.7687	0.3504	-8.44
59	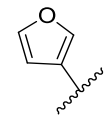	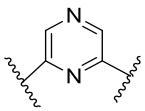	-	-	4.9219	0.2882	-7.99
60	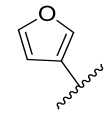	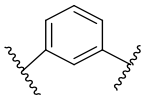	-	-	4.8167	0.4578	-8.69
61	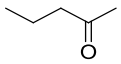	-	-	-	5.0779	0.3122	-8.99
62	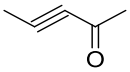	-	-	-	5.1376	0.1791	-9.10
63	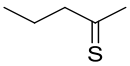	-	-	-	5.4350	0.5566	-9.40
64	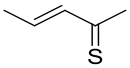	-	-	-	5.5407	0.4983	-9.51
65	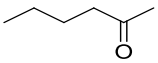	-	-	-	4.9316	0.3974	-9.80
66	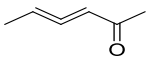	-	-	-	5.1054	0.2331	-9.31
67	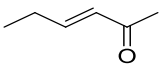	-	-	-	5.0156	0.3512	-9.79
68	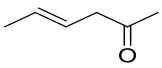	-	-	-	4.9658	0.3190	-9.46
69	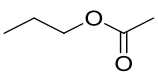	-	-	-	4.9119	0.2212	-9.02
70	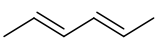	-	-	-	4.6693	0.1043	-9.66

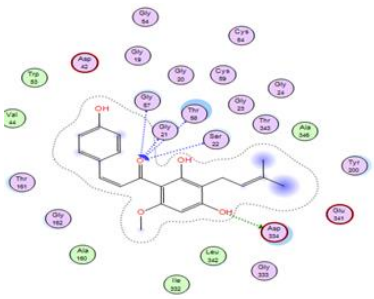
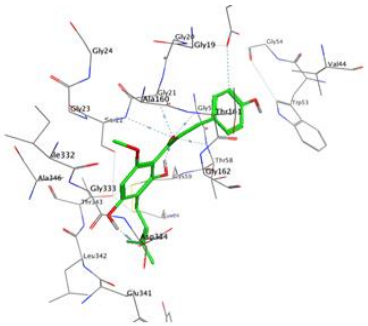

8a

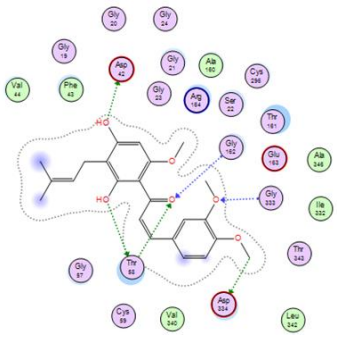
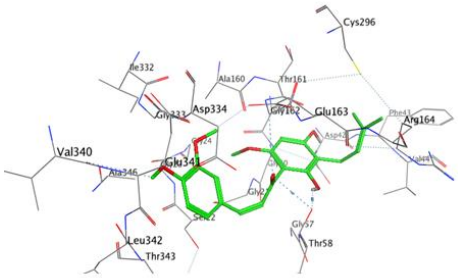

8f

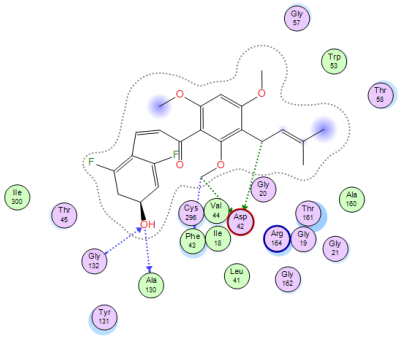
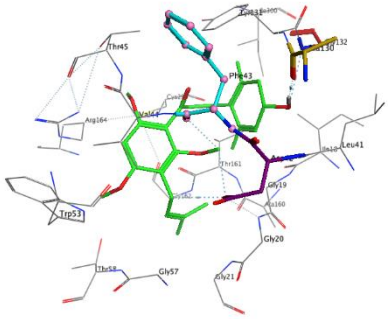

30

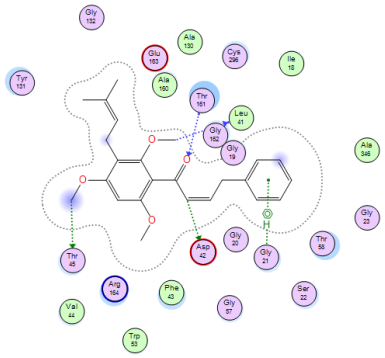
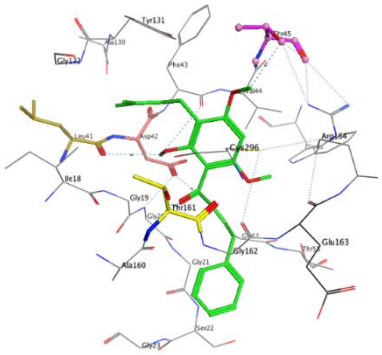

67

Figure 1. The structures of 2D and 3D of **8a**, **8f**, **30** and **67** surrounded by the key residues in the active site of TrxRS (3QFB)

The results show that the important amino acids inside the active site cavity which have essential interactions with tubulin are Thr58, Gly57, Gly21, Asp334, Glu163, Ala130, iie332, Val44 and Gly132.

The use of the relative performance characteristic curve (ROC) is a useful metric tool that calculates the weight of the procedure for docking methods [29, 30]. Initially the chembl database was retrieved as SMILES format [31-33] for about 82 TrxR inhibitors. Based on the experimental activities, the structures are classified into two categories of active ligands and inactive decoys. 17 ligands and 65 creams were produced for TrxR. Subsequently, through a shell script using openbabel 2.3.2, an initial generation of structural structure was presented as mol2 mold [34]. Also, all structures were calculated in ionization conditions at pH = 7.

Using batch scripting in windows operating system, the shell script was obtained. This screening method should be able to discriminate between active ligands and inactive decoys. ROC value is the area under the curve (AUC) for the plot of the true positive rate (TPR or sensitivity) against the false positive rate (FPR or 1-specificity) at various threshold settings. The ROC curve is thus the sensitivity as a function of 1-specificity. The AUC for ROC is calculated by trapezoidal integration method as implemented in our in house ROC application [35]. The larger AUC value means that the docking protocol is more capable to discriminate between ligands and decoys.

Figure 2 certificates the AUC of 0.7 for TrxR and our applied docking protocol was a validated protocol. On the other hand, to evaluate the efficiency and quality of docking protocol with another tool, Enrichment Factor (efmax). based on the Li *et al*. [36] was used. Efmax factor in comparison to ROC curves, is highly dependent on the number of actives in a data set [29]. It means that early enrichment can be easily obtained if the number of active ligands is increasing in a dataset. Hence, the ROC should be considered most importantly.

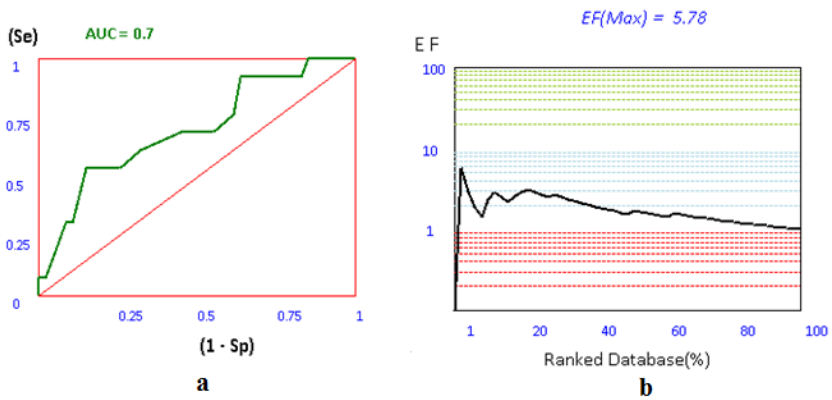

Figure 2. a) ROC and b) EF diagrams for docking with TrxRS

Conclusion

Based on the developed QSAR model, *in silico* screening was done and new compounds such as **16**, **19**, **21**, **25**, **26**, **27-30**, **32**, **33**, **35**, **36**, **39**, **40**, **42**, **44**, **46**, **50-54** and **62-70** with potential Cytotoxicity activity were suggested for the synthesis. To take into account the molecular binding mode with TrxR as their target and to elucidate their

interactions, molecular docking simulations were also done on these compounds. The important amino acids inside the active site cavity which have essential interactions with tubulin are Thr58, Gly57, Gly21, Asp334, Glu163, Ala130, iie332, Val44 and Gly132.

Acknowledgements
The authors want to thank the research deputy of Payame Noor University of Isfahan who supported this work.

References

[1] C. Gerhauser, *Eur. J. Cancer*, **2005**, *41*, 1941−1954.
[2] M.M. Blanquer-Rossello, J. Oliver, A. Valle, P. Roca, *J. Cell. Biochem*., **2013**, *114*, 2785−2794.
[3] M. Festa, A. Capasso, C.W. Dacunto, M. Masullo, A.G. Rossi, C. Pizza, S. Piacente, *J. Nat. Prod*., **2011**, *74*, 2505−2513.
[4] J. Strathmann, K. Klimo, S.W. Sauer, J.G. Okun, J.H. Prehn, C. Gerhäuser, *FASEB J.*, **2010**, *24*, 2938−2950.
[5] Y. Kang, M.A. Park, S.W. Heo, S.Y. Park, K.W. Kang, P.H. Park, J.A. Kim, *Biochim. Biophys. Acta*, **2013**, *1830*, 2638−2648.
[6] D. Deeb, X. Gao, H. Jiang, A.S. Arbab, S.A. Dulchavsky, S.C. Gautam, *Anticancer Res*., **2010**, *30*, 3333−3339.
[7] K.B. Harikumar, A.B. Kunnumakkara, K.S. Ahn, P. Anand, S. Krishnan, S. Guha, B.B. Aggarwal, *Blood*, **2009**, *113*, 2003−2013.
[8] A. Albini, R. Dell'Eva, R. Vené, N. Ferrari, D.R. Buhler, D.M. Noonan, G. Fassina, *FASEB J*., **2006**, *20*, 527−529.
[9] S. Monteghirfo, F. Tosetti, C. Ambrosini, S. Stigliani, S. Pozzi, F. Frassoni, G. Fassina, S. Soverini, A. Albini, N. Ferrari, *Mol. Cancer Ther*., **2008**, *7*, 2692−2702.
[10] H. Becker, C. Gerhauser, *Mol. Nutr. Food Res*., **2005**, *49*, 837−843.
11] C. Gerhauser, A. Alt, E. Heiss, A. Gamal-Eldeen, K. Klimo, J. Knauft, I. Neumann, H.R. Scherf, N. Frank, H. Bartsch, H. Becker, *Mol. Cancer Ther*., **2002**, *1*, 959−969.
[12] C.I. Miranda, G.L. Aponso, J.F. Stevens, M.L. Deinzer, D.R. Buhler, *Cancer Lett.*, **2000**, *149*, 21−29.
[13] T.C. Laurent, E.C. Moore, P. Reichard, *J. Biol. Chem*., **1964**, *239*, 3436–3444.
[14] E.C. Moore, P. Reichard, L. Thelander, *J. Biol. Chem*., **1964**, 239, 3445–3452.
[15] A. Holmgren, *Eur. J. Biochem*., **1968**, *6*, 475–484.
[16] A. Holmgren, B.O. Soderberg, H. Eklund, C.I. Branden, *Proc. Natl. Acad. Sci. USA*, **1975**, *72*, 2305–2309.
[17] L. Zhang, D. Duan, Y. Liu, C. Ge, X. Cui, J. Sun, J. Fang, *J. Med. Chem.,* **2015***,* 58, 1795−1805.
[18] S. Urig, K. *Semin. Cancer Biol.*, **2006**, *16*, *452*-465.
[19] X.Y. Meng, H.X. Zhang, M. Mezei, M. Cui, *Curr. Comput. Aided Drug Des.*, **2011**, *7*, 146–157.
[20] S. Zare, M. Fereidoonnezhad, D. Afshar, Z. Ramezani, *Comput. Biol. Chem.*, **2017**, *67*, 22-37.
[21] A. Mojaddami, A. Sakhteman, M. Fereidoonnezhad, Z. Faghih, A. Najdian, S. Khabnadideh, H. Sadeghpour, Z. *Res. Pharm. Sci.*, **2017**, *12*, 21-30.
[22] HyperChem(TM) Professional 8.0 Hypercube Inc. 1115 NW 4th Street Gainesville Florida 32601 USA.
[23] G.M. Morris R. Huey, A.J. Olson, Using AutoDock for Ligand-Receptor Docking. Current Protocols in Bioinformatics: John Wiley & Sons Inc, **2002**.
[24] G.M. Morris, D.S. Goodsell, R.S. Halliday, R. Huey, W.E. Hart, R.K. Belew, A.J. Olson, *J. Comput. Chem.*, **1998**, *19*, 1639-1662.

[25] A. Hamedi, M.J. Khoshnoud, N. Tanideh, F. Abbasi, M. Fereidoonnezhad, D. Mehrabani, *Pharm. Chem. J.*, **2015**, *49*, 268-274.
[26] W. Humphrey, A. Dalke, K. Schulten, *J. Mol. Graphics*, **1996**, *14*, 33-38.
[27] W.L. DeLano, PyMOL: An open-source molecular graphics tool. Delano Scientific San Carlos. **2002**.
[28] M. Oftadeh, M. Fereidoonnezhad, M. Aliyan, F. Aliyan, *Phys. Chem. Res.*, under review.
[29] N. Triballeau, F. Acher, I. Brabet, P.J. Pin, H.O. Bertrand, *J. Med. Chem.*, **2005**, *48*, 2534-2547.
[30] Z. Rezaei, M. Fereidoonnezhad, Z. Faghih, H. Sadeghpur, A. Mojaddami, A. Sakhteman, *Trends Pharm. Sci.*, **2017**, *3*, 31-42.
[31] A. Gaulton, L.J. Bellis, A.P. Bento, J. Chambers, M. Davies, A. Hersey, Y. Light, S. McGlinchey, D. Michalovich, B. Al-Lazikani, J.P. *Nucleic Acids Res.*, **2012**, *40*, D1100–D1107.
[32] A.M. Wassermann, J. Bajorath, *Expert Opin. Drug Dis.*, **2011**, *6*, 683-687.
[33] E.L. Willighagen, A. Waagmeester, O. Spjuth, P. Ansell, A.J. Williams, V. Tkachenko, J. Hastings, B. Chen, D.J. Wild, *J. Cheminform.*, **2013**, *5*, 23-28.
[34] N.M. O'Boyle, M. Banck, C.A. James, C. Morley, T. Vandermeersch, G.R. Hutchison, *J. Cheminform.*, **2011**, *3*, 33-43.
[35] K. Roy, S. Kar, R.N. Das, Validation of QSAR Models. Understanding the Basics of QSAR for Applications in Pharmaceutical Sciences and Risk Assessment Academic Press: Boston, **2015**, pp. 231-89.
[36] H. Li, H. Zhang, M. Zheng, J. Luo, L. Kang, X. Liu, X. Wang, H. Jiang, *BMC Bioinformatics*, **2009**, *10*, 58-60.

How to cite this manuscript: Mohsen Oftadeh, Masood Fereidoonnezhad, Mina Aliyan, Fariba Aliyan. Molecular docking studies on xanthohumol derivatives as novel anticancer agents. *Iranian Chemical Communication*, 2019, 7(4), 272-284.